AD-A112 783 OHIO STATE UNIV COLUMBUS ELECTROSCIENCE LAB F/G 20/14
ANALYSIS OF AIRCRAFT SIMULATIONS USING AN ELLIPTIC CYLINDER AND--ETC(U)
APR 79 W D BURNSIDE, N WANG, E L PELTON N00019-78-C-0524
UNCLASSIFIED ESL-711305-1 NL

1 OF 1
AD A
112783

END
DATE
FILMED
04-82
DTIC

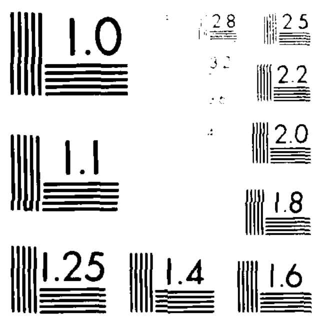
1.0
2.8
2.5
2.2
2.0
1.1
1.8
1.25
1.4
1.6

①

OSU

ANALYSIS OF AIRCRAFT SIMULATIONS USING AN ELLIPTIC CYLINDER AND MULTIPLE PLATES

W.D. Burnside, N. Wang and E.L. Pelton

AD A112 ... 3

The Ohio State University

ElectroScience Laboratory

Department of Electrical Engineering
Columbus, Ohio 43212

QUARTERLY REPORT 711305-1

April 1979

Contract N00019-78-C-0524

Department of the Navy
Naval Air Systems Command
Washington, D.C. 20361

NOTICES

When Government drawings, specifications, or other data are used for any purpose other than in connection with a definitely related Government procurement operation, the United States Government thereby incurs no responsibility nor any obligation whatsoever, and the fact that the Government may have formulated, furnished, or in any way supplied the said drawings, specifications, or other data, is not to be regarded by implication or otherwise as in any manner licensing the holder or any other person or corporation, or conveying any rights or permission to manufacture, use, or sell any patented invention that may in any way be related thereto.

UNCLASSIFIED

SECURITY CLASSIFICATION OF THIS PAGE (When Data Entered)

REPORT DOCUMENTATION PAGE

READ INSTRUCTIONS BEFORE COMPLETING FORM

1. REPORT NUMBER	2. GOVT ACCESSION NO. AD-A112 783	3. RECIPIENT'S CATALOG NUMBER
4. TITLE (and Subtitle) ANALYSIS OF AIRCRAFT SIMULATIONS USING AN ELLIPTIC CYLINDER AND MULTIPLE PLATE		5. TYPE OF REPORT & PERIOD COVERED Quarterly Report
		6. PERFORMING ORG. REPORT NUMBER ESL 711305-1
7. AUTHOR(s) W.D. Burnside, E.L. Pelton, N. Wang		8. CONTRACT OR GRANT NUMBER(s) Contract N00019-78-C-0524
9. PERFORMING ORGANIZATION NAME AND ADDRESS The Ohio State University ElectroScience Laboratory, Department of Electrical Engineering Columbus, Ohio 43212		10. PROGRAM ELEMENT, PROJECT, TASK AREA & WORK UNIT NUMBERS
11. CONTROLLING OFFICE NAME AND ADDRESS Department of the Navy Naval Air Systems Command Washington, D.C. 20361		12. REPORT DATE April 1979
		13. NUMBER OF PAGES 26
14. MONITORING AGENCY NAME & ADDRESS(if different from Controlling Office)		15. SECURITY CLASS. (of this report) Unclassified
		15a. DECLASSIFICATION/DOWNGRADING SCHEDULE

16. DISTRIBUTION STATEMENT (of this Report)

APPROVED FOR PUBLIC RELEASE
DISTRIBUTION UNLIMITED

17. DISTRIBUTION STATEMENT (of the abstract entered in Block 20, if different from Report)

18. SUPPLEMENTARY NOTES

19. KEY WORDS (Continue on reverse side if necessary and identify by block number)

Near field patterns
Aircraft substructures
Multiplate simulations
High frequency analysis
Geometrical theory of diffraction
Efficient numerical solution

20. ABSTRACT (Continue on reverse side if necessary and identify by block number)

The aircraft simulation model developed under previous contract (N00019-77-0299) is extended in an attempt to study the pattern effects due to the presence of various substructures attached to an aircraft. A simple, efficient multiplate model is developed in that the various substructures, such as the jet engine housing, are treated simply by boxing-out the shape using multiple finite plates. This new numerical solution with second-order interaction GTD terms included shows excellent agreement when compared with the measured results.

DD FORM 1 JAN 73 1473 EDITION OF 1 NOV 65 IS OBSOLETE

UNCLASSIFIED

SECURITY CLASSIFICATION OF THIS PAGE (When Data Entered)

TABLE OF CONTENTS

I. INTRODUCTION

Under our previous contract (N00019-77-C-0299) an aircraft simulation model was developed which treated the fuselage as a composite elliptic cylinder and the wings and stablizers as finite flat plates. That numerical solution was based on a near field formulation as presented in Reference 1 such that one could compute the pattern at a finite range. As the previous solution was used to analyze various private, commercial, and military aircraft, it became apparent that it had several shortcomings which had to be corrected before it would be really useful for a general aircraft problem. The main objection with the previous solution was in its inability to simulate arbitrary structures which might be attached to the basic aircraft. For private aircraft, there was no way with the previous model to simulate wing tanks, engine housings, propellors, etc. For commercial aircraft, one could not treat "T"-tail aircraft, jet engine housings, etc. For military aircraft, one can easily visualize numerous structures being attached to the basic fuselage and wing. For these reasons, the previous numerical solution of Reference 1 is to be extended under the present contract to treat multiple plates which can be attached to the fuselage or not, as well as being attached or not to other plates. Using this multiple plate approach, one can treat wing tanks, engine housing, T-tails, etc. simply by boxing-out the structure using finite flat plates. The finite plate models were chosen to simulate these structures in that they are easy to input in the code and are much more efficient to analyze. The validity of the flat plate simulations will be studied under the present contract as well as others which might wish to use the code to treat a special application. Note that under this contract, the general near field aircraft code is being developed and tested for simple models. Specific applications of the code will be done as the need arises on various other contracts. For example, it has been used to analyse private aircraft configurations for NASA as reported in Reference 2.

II. VARIOUS GTD TERMS

In order to illustrate how the present solution is developed based on our analysis, a set of problems are presented which illustrate the different GTD mechanisms included in the solution. The first example illustrates the GTD mechanisms used in our previous analysis. For this purpose a single flat plate is attached to a circular cylinder as shown in Figure 1. The various terms treated using the previous solution

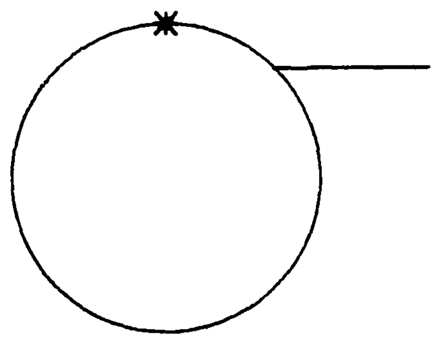

Figure 1. A flat plate attached to a circular cylinder.

are shown in Figure 2. Note that each pattern is normalized to the same level such that one can see the relative significance of each term. In order to better observe how the total Geometrical Theory of Diffraction (GTD) solution evolves, various terms are superimposed in Figure 3. Note that the double diffraction term is being introduced to the solution under the present effort. An interesting result is shown in Figure 3a where the source and reflected fields are superimposed. These two terms form the classical "Geometrical Optics" (GO) solution. However, one should note that the GO solution is far from complete as can be observed from the discontinuities in the pattern. Our final GTD solution shown in Figure 3d is seen to be continuous and should agree with experimental as verified by several examples given in Reference 1.

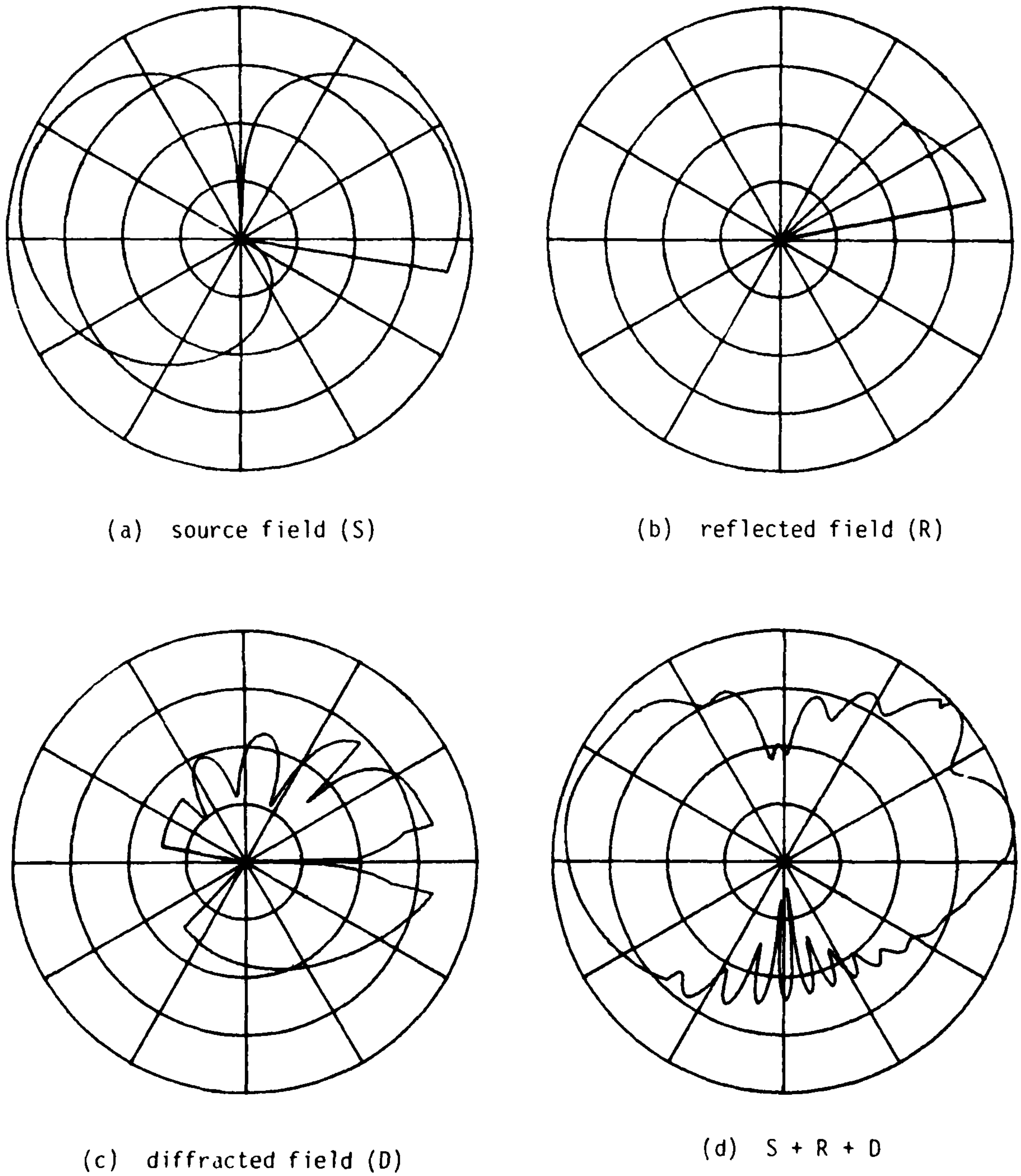

Figure 2. Radiation patterns due to various ray mechanisms.

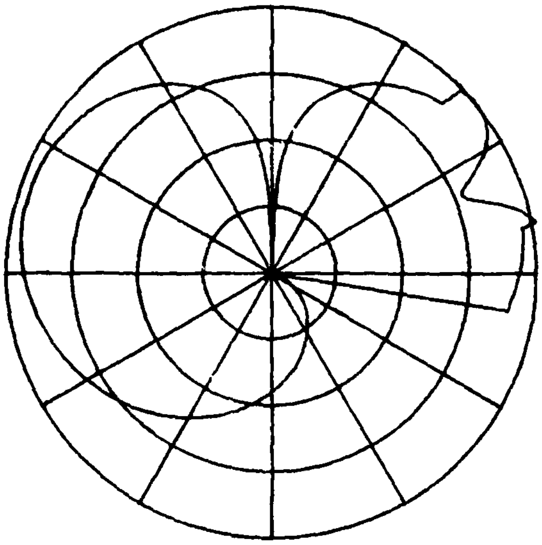

(a) S + R

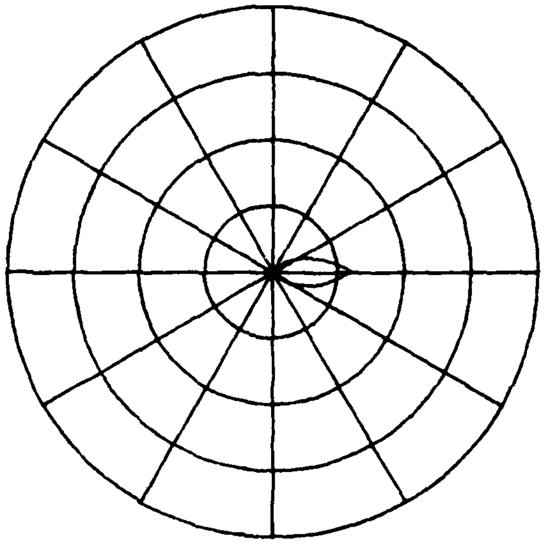

(b) double diffracted field (D/D)

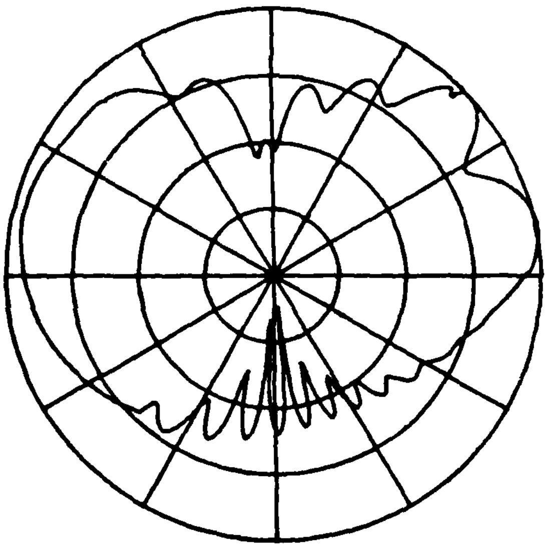

(c) S + R + D

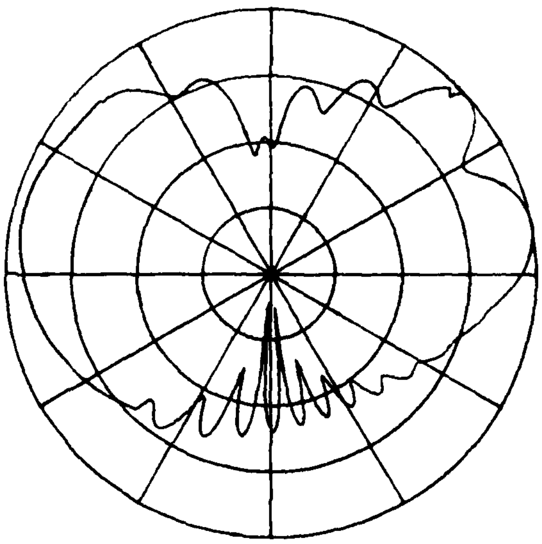

(d) S + R + D + D/D

Figure 3. Radiation patterns due to various combinations of the GTD terms.

The next example is used to illustrate the additional GTD mechanisms added under the present contract. This geometry is shown in Figure 4 in which a second plate is added to the model discussed in

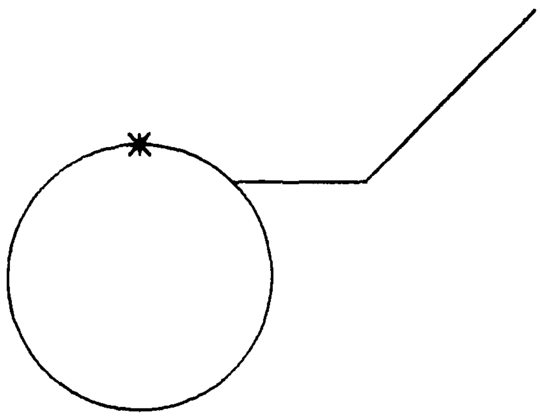

Figure 4. A bent plate attached to a circular cylinder.

the previous paragraph. The source, reflected, and diffracted terms used in our previous solution are shown in Figure 5. The superimposed pattern using these three GTD terms is illustrated in Figure 5d. One should note the discontinuities in this pattern at $\simeq 14^{\circ}$ and 45°. These discontinuities are compensated for by the higher-order GTD interaction terms illustrated in Figure 6. As before, these terms are plotted relative to the same signal level such that one can observe their relative significance. It is clear that these higher-order terms can be significant in certain sectors of the pattern. In order to demonstrate how the complete GTD solution creates the desired total pattern, various combinations of terms are illustrated in Figure 7. The GO solution is shown in Figure 7b and, as before, several discontinuities exist in this pattern. The total superposition of the recently introduced higher-order terms is shown in Figure 7c. It is very interesting that the patterns illustrated in Figure 7b and c superimpose to give the total pattern shown in Figure 7d. As with any GTD solution for a complex structure, one can compute higher- and higher-order terms. However,

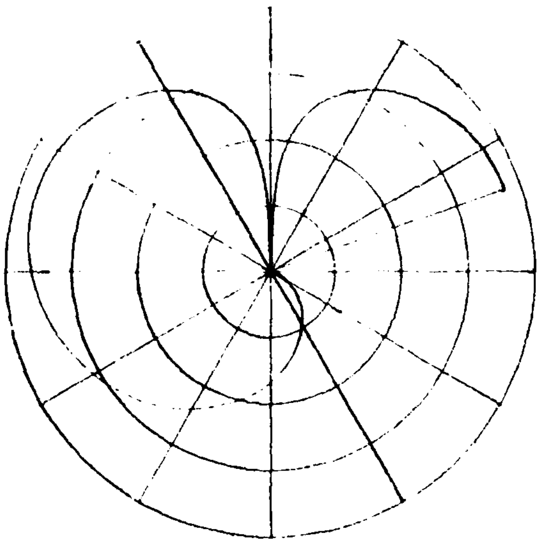

(a) source field (S)

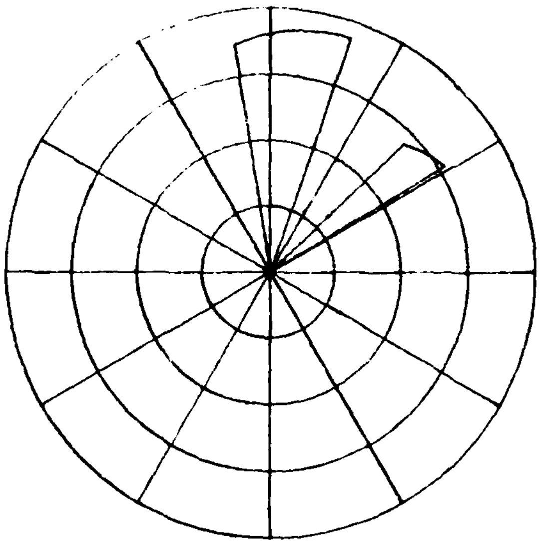

(b) reflected field (R)

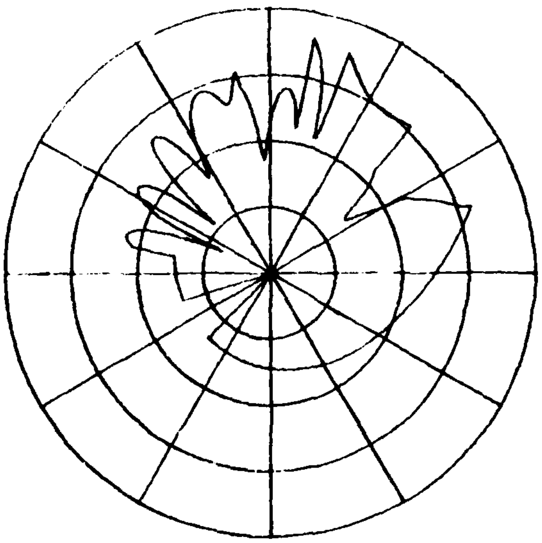

(c) diffracted field (D)

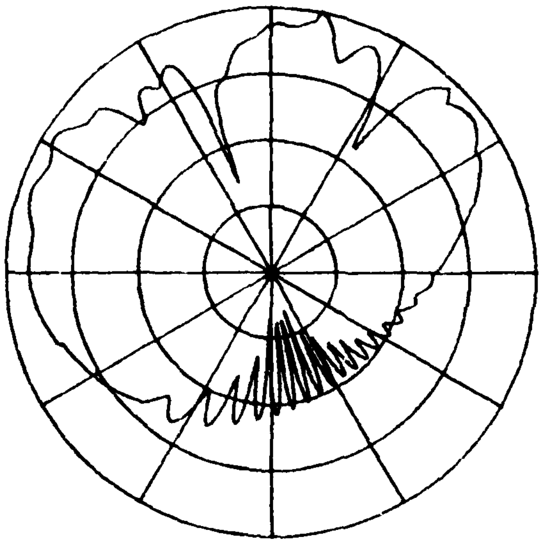

(d) S + R + D

Figure 5. Radiation patterns due to various GTD terms.

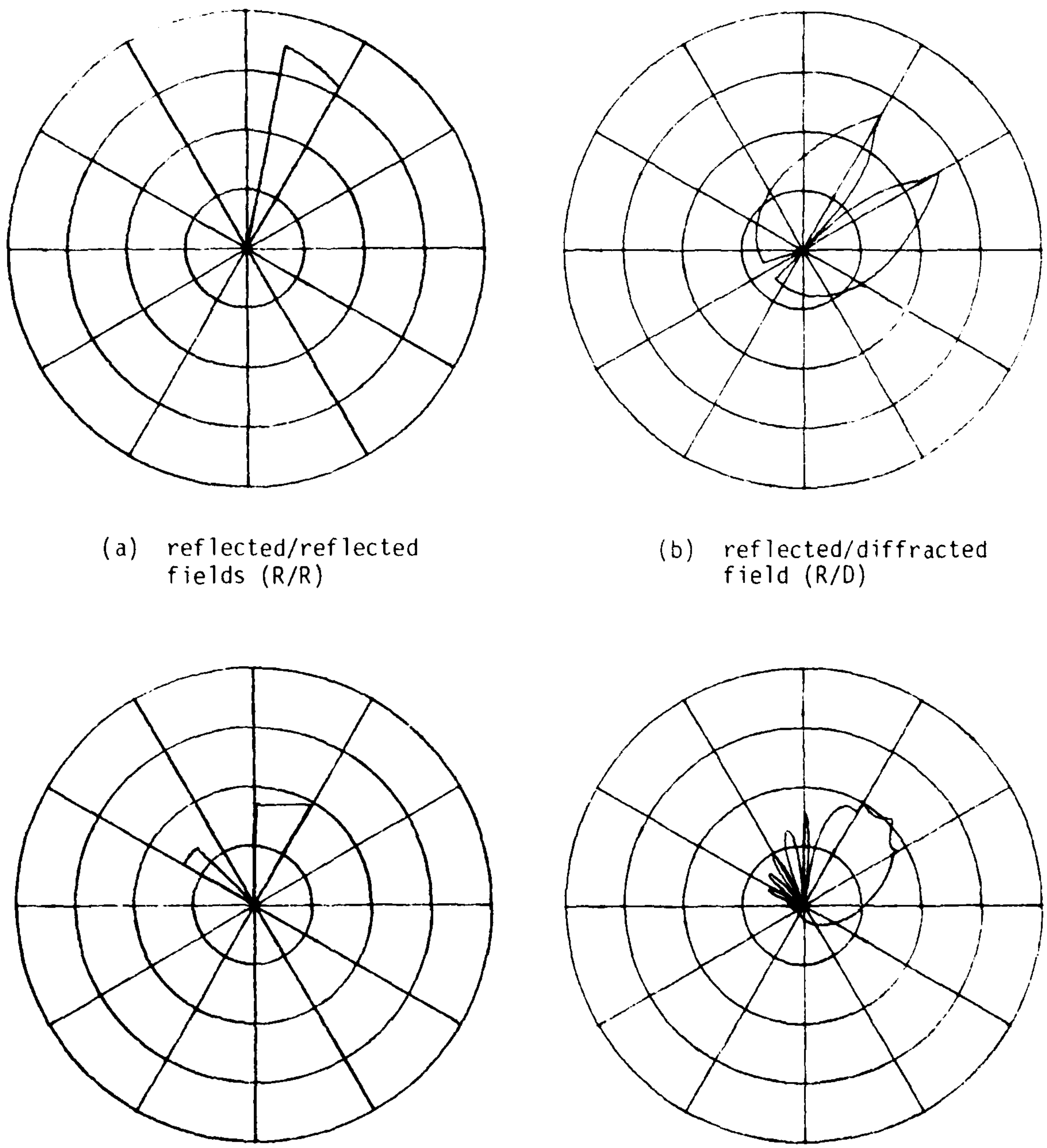

(a) reflected/reflected fields (R/R)

(b) reflected/diffracted field (R/D)

(c) diffracted/reflected field (D/R)

(d) diffracted/diffracted field (D/D)

Figure 6. Radiation patterns due to the second order interaction GTD terms.

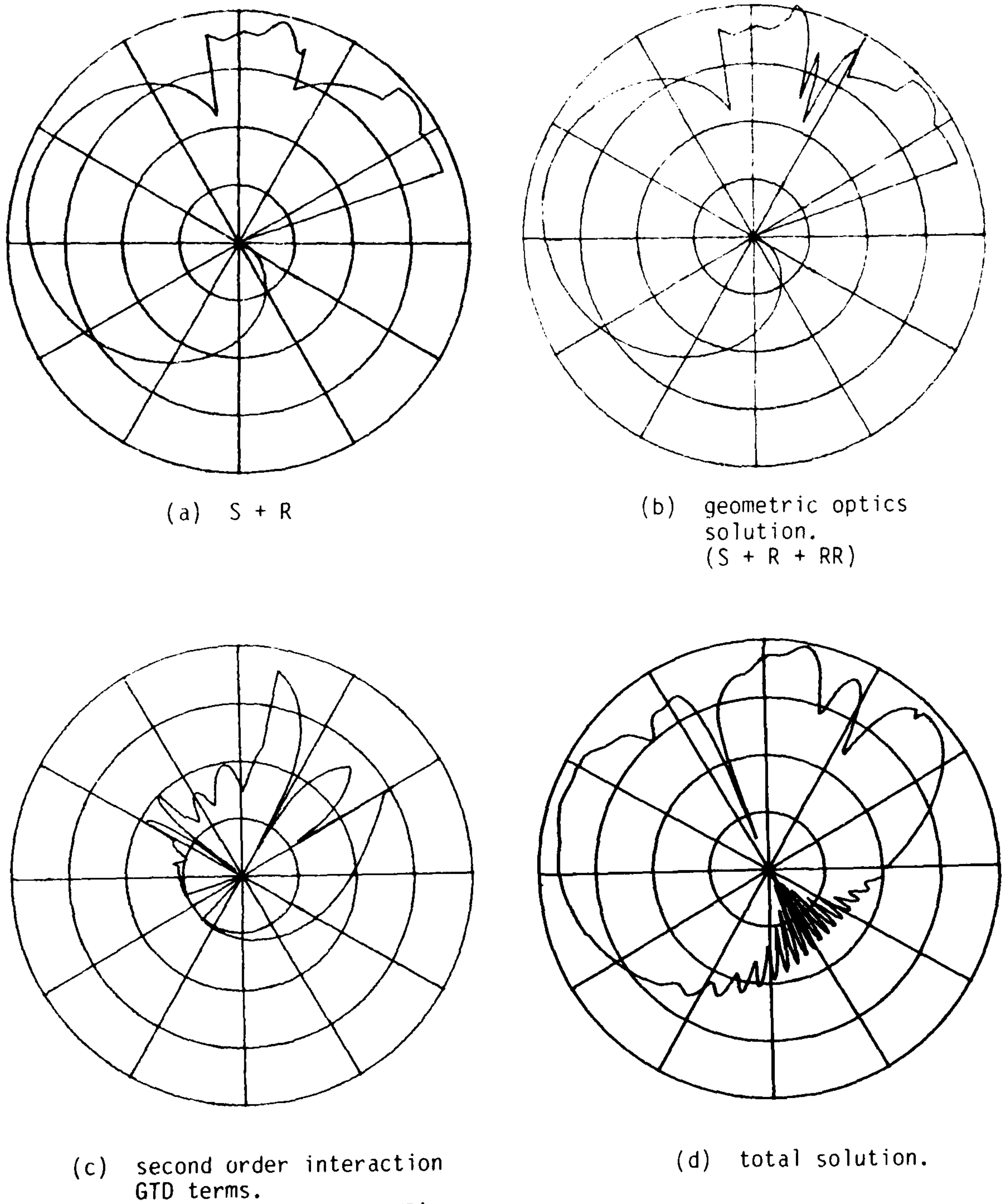

(a) S + R

(b) geometric optics solution. (S + R + RR)

(c) second order interaction GTD terms. (R/R + R/D + D/R + D/D)

(d) total solution.

Figure 7. Radiation patterns due to various combinations of the GTD terms.

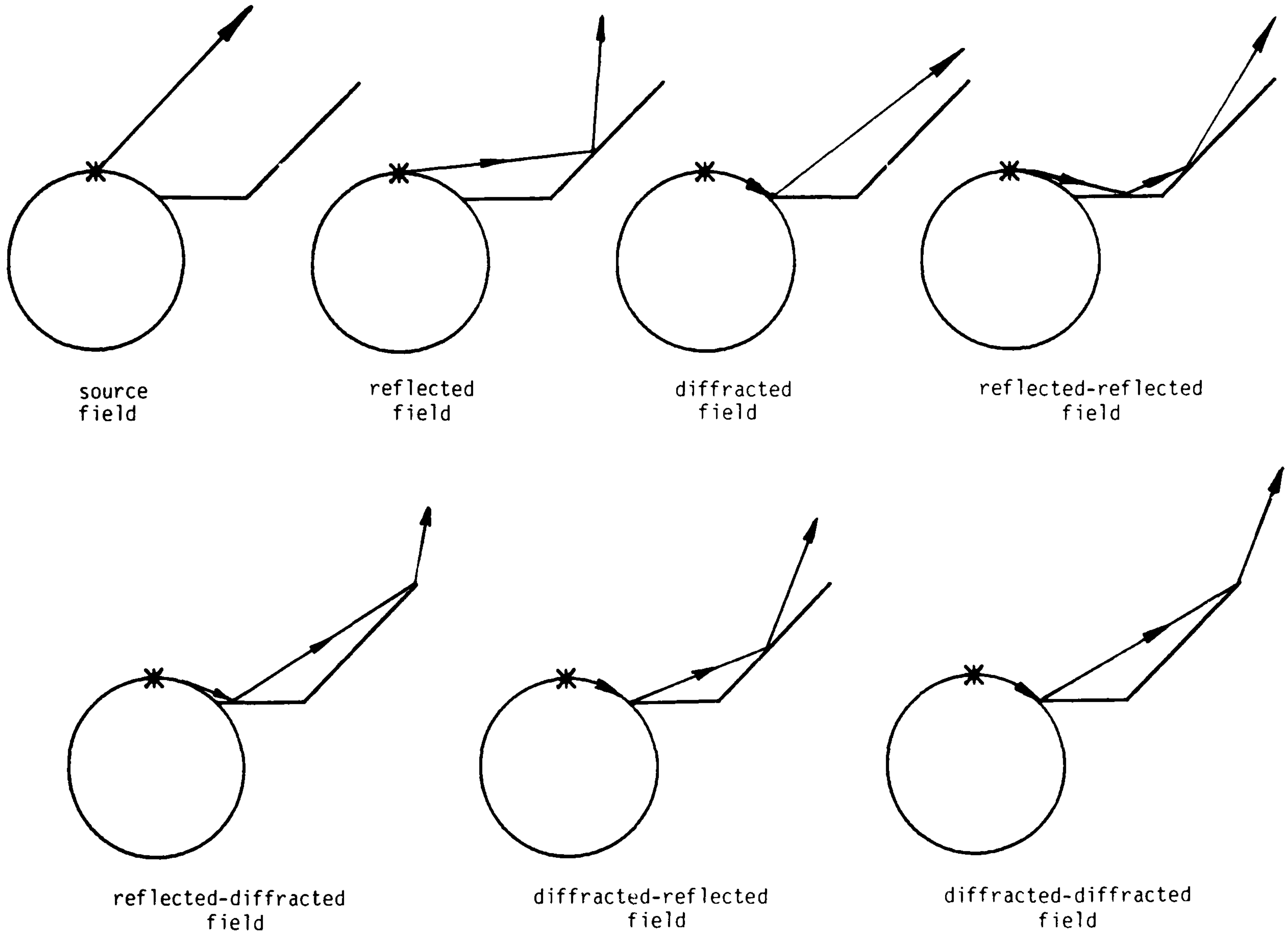

Figure 8. Various GTD terms.

there are two major problems with adding such terms beyond those included here: 1) The accuracy of the GTD diffraction solutions become questionable, 2) The numerical solution becomes very inefficient. Furthermore based on cases examined to date, it appears that the major structures found on aircraft can be adequately solved using the interaction terms considered here. In order to illustrate the various GTD mechanisms they are all shown in Figure 8 in terms of ray paths.

The previous example was used to illustrate the various higher-order terms used in the present analysis. This next problem is used to show the various GTD terms for a more realistic geometry as shown in Figure 9. In this case, additional plates are added which might be used to

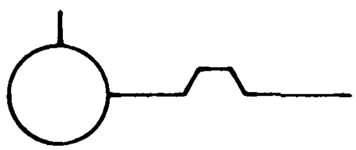

Figure 9. Flat plate model for the wing and the engine.

simulate the engine housing for a private aircraft. The first-order terms (source, reflected, and diffracted) are shown in Figure 10. The second-order interaction terms are shown in Figure 11, and they represent the modification to the analysis made under the present contract. Finally, various combinations of GTD terms are illustrated in Figure 12. Again, it is very interesting how all the different discontinuous GTD terms combine to give the nice smooth total pattern shown in Figure 12d.

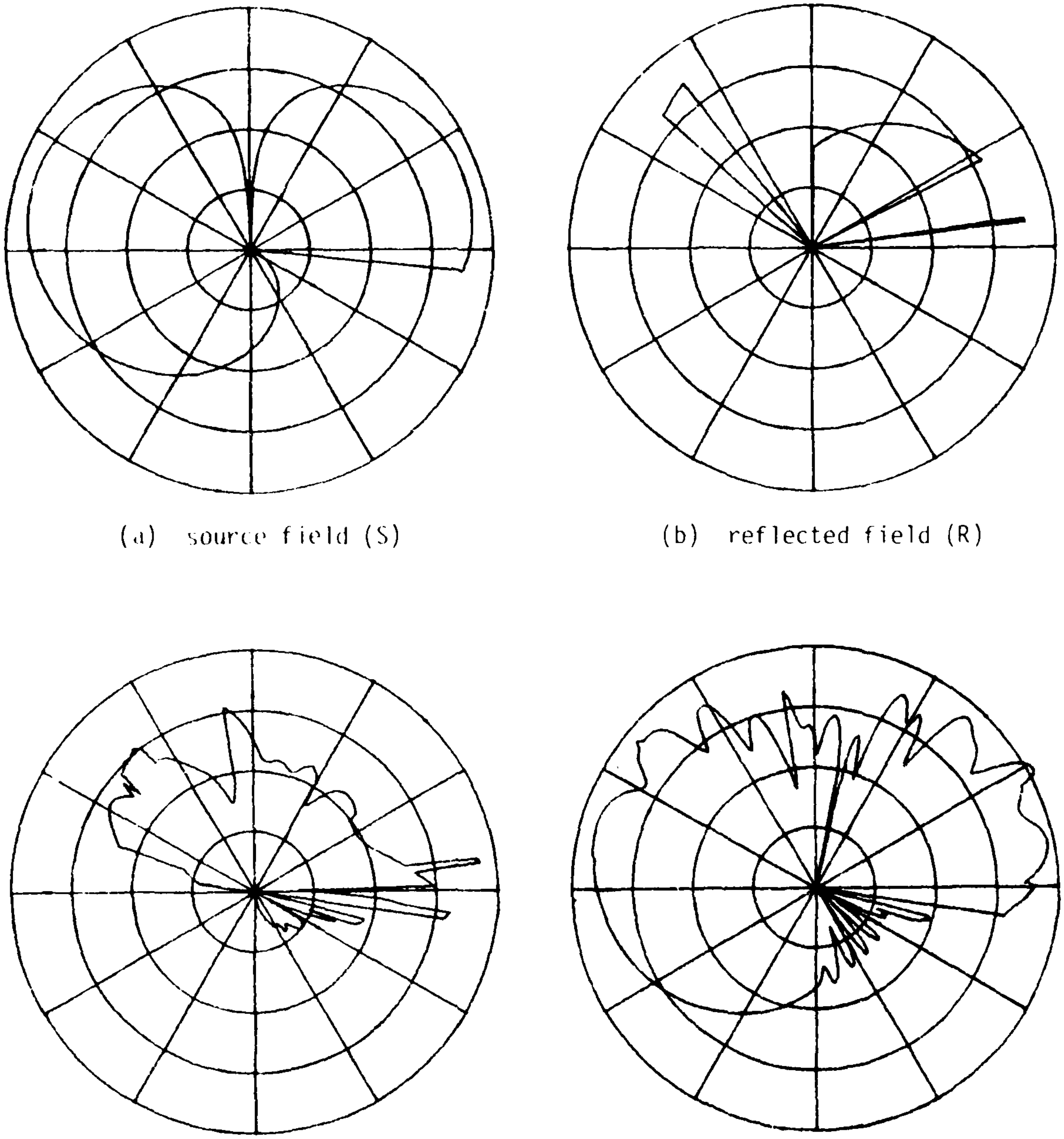

(a) source field (S)

(b) reflected field (R)

(c) diffracted field (D)

(d) S + R + D

Figure 10. Radiation patterns due to various GTD terms.

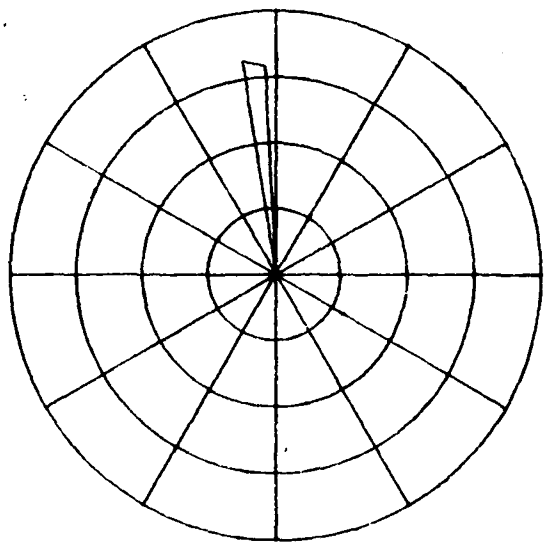

(a) reflected/reflected field (R/R)

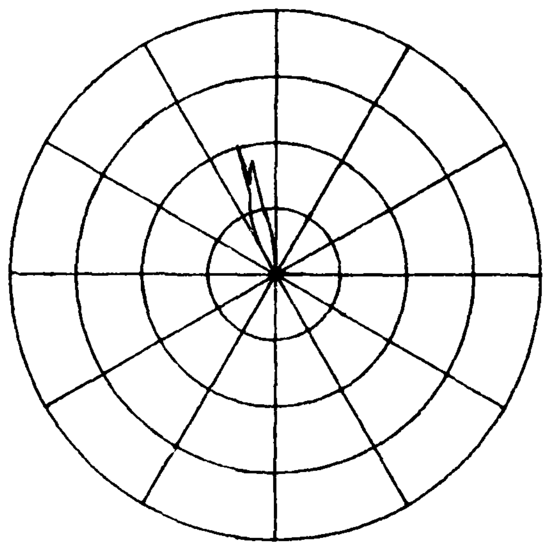

(b) reflected/diffracted field (R/D)

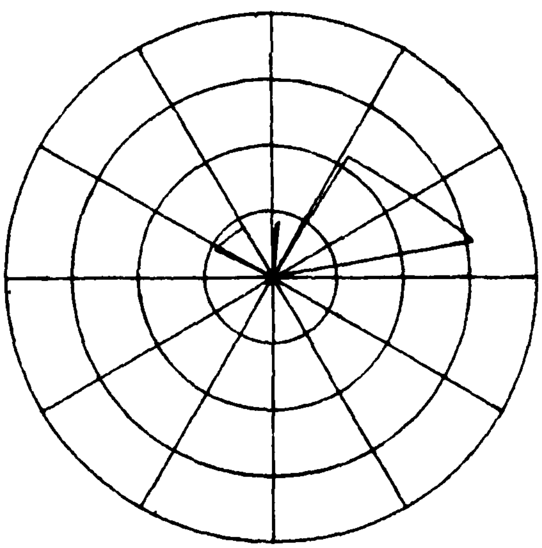

(c) diffracted/reflected field (D/R)

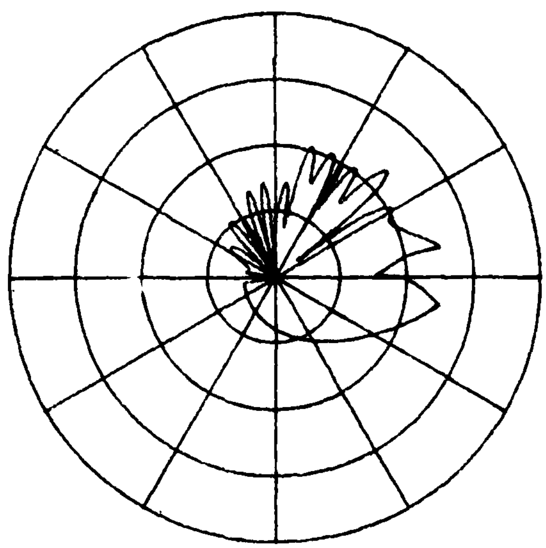

(d) diffracted/diffracted field (D/D)

Figure 11. Radiation patterns due to the second order iteration GTD terms.

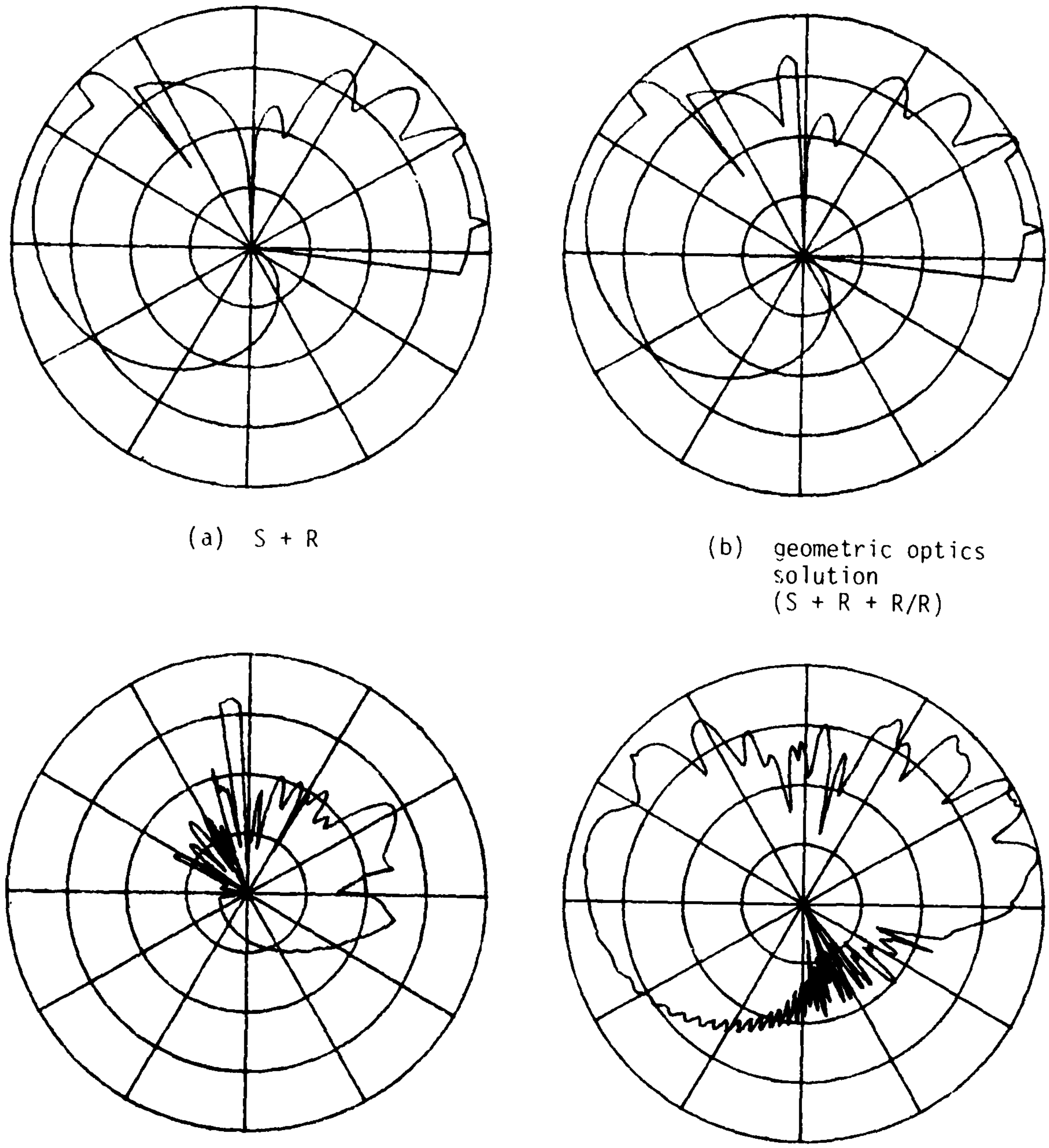

(a) S + R

(b) geometric optics solution (S + R + R/R)

(c) second order interaction GTD terms (R/R + R/D + D/R + D/D)

(d) total solution

Figure 12. Radiation patterns due to various combinations of the GTD terms.

III. EXPERIMENTAL VERIFICATION

Since new structures are being treated under the present contract, some experimental verification is necessary. As stated previously, this verification is only done using the simpler multiple plate structures. No attempt will be made here by us to measure scale models of actual aircraft configurations. This is merely an attempt to verify that our numerical solution is accurate for the simpler multiple plate structures. Comparison with scale model measurements will be done on other contracts such as the private aircraft simulations done in Reference 2.

The first example is used to verify our numerical solution for the last configuration of the previous section. The calculated and measured roll plane patterns are shown in Figure 13. In the next case, the engine plate model is slid out the wing. The measured and calculated roll plane patterns for this geometry are shown in Figure 14. In each case, excellent agreement between measured and calculated results is obtained.

The final example considered here is illustrated in Figure 15. This geometry is included in that it tends to resemble a more realistic aircraft configuration. The roll plane measured and calculated patterns are shown in Figure 16. Two sets of measured and calculated patterns are illustrated in Figures 17 and 18 for 68^{o} and 112^{o} conical pattern cuts. In each case both the E_θ and E_ϕ components of the near zone field are plotted relative to the same radiation level. In each case, there is very good agreement between calculated and measured patterns.

The above patterns are presented to illustrate that our numerical solutions can solve the proposed type of airborne antenna problem. It is the first step in the complete verification process. The next step is to apply the code to numerous practical airborne antenna problems

and ascertain its limits, shortcomings, and possible improvements. As stated earlier, this step is presently being accomplished under other contracts. The significant results of those findings will be reported later. In any event, it appears that the present solution does adequately simulate the engine housings, wing tanks, "T" tails, etc. for which it was intended.

Note that all the input data used for the test geometries are given in the Appendix. In addition, all the previous polar plots are illustrated in terms of decibels with 10 dB per major division.

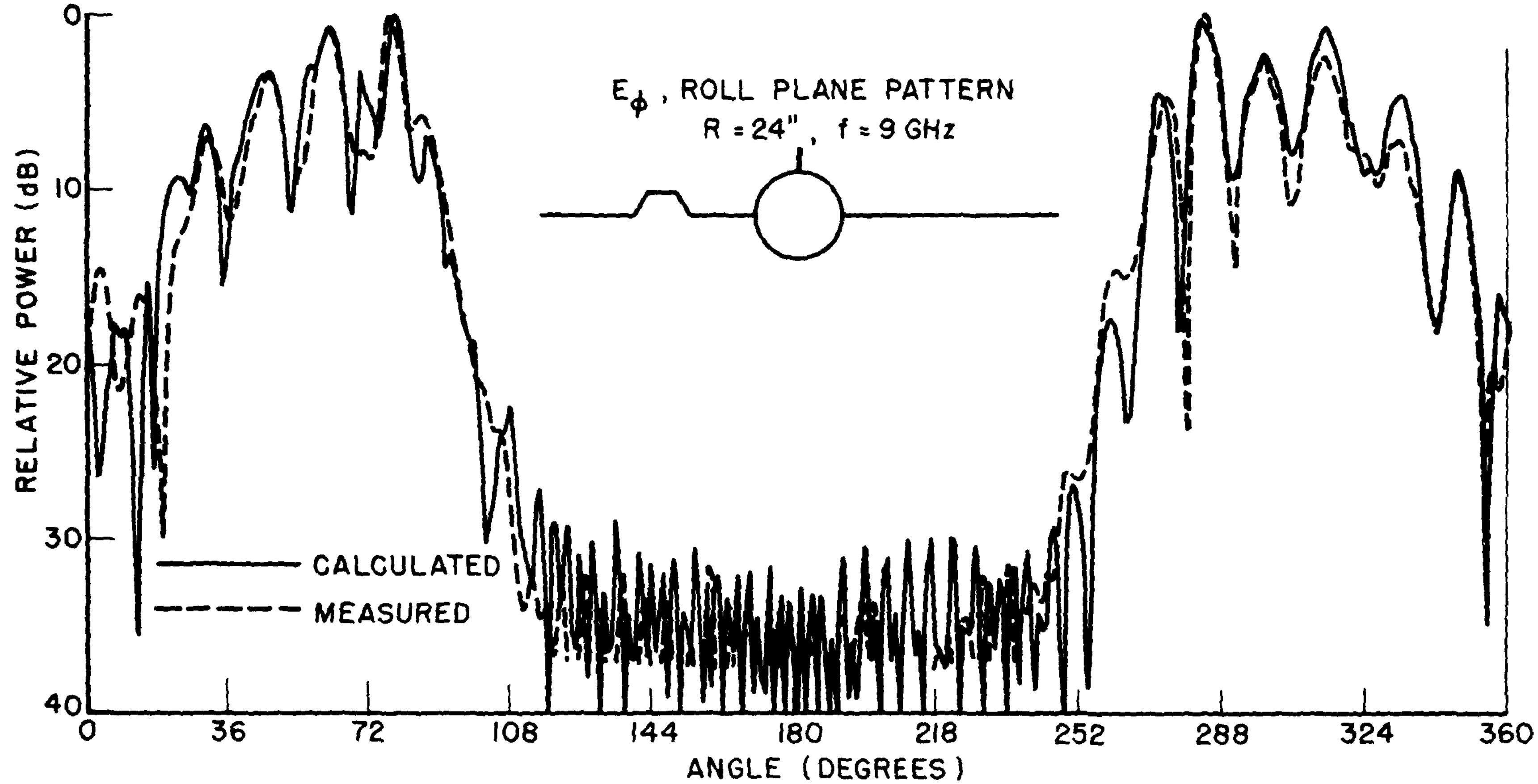

Figure 13. Comparison of measured and calculated near-field pattern for the test geometry shown.

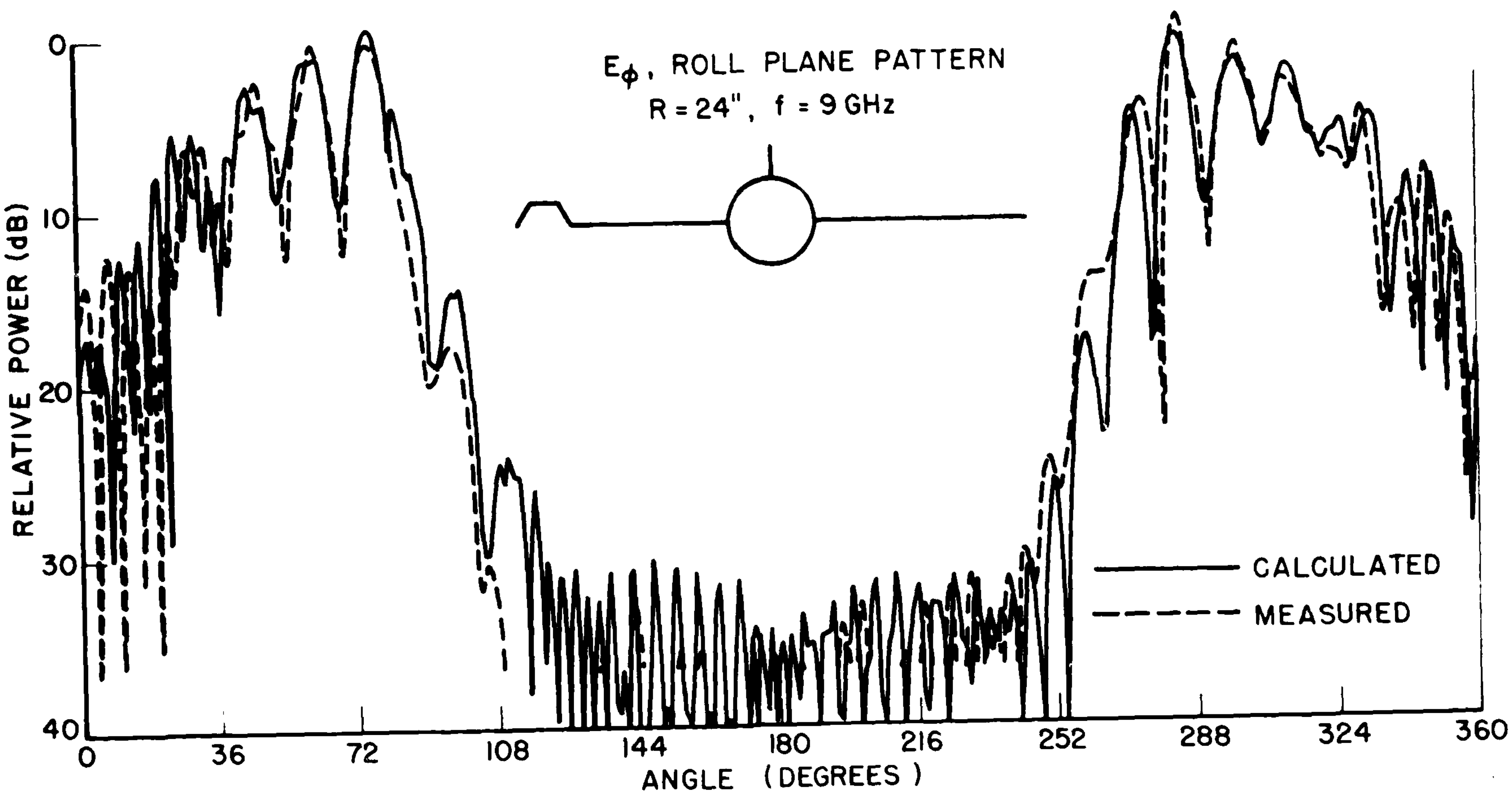

Figure 14. Comparison of measured and calculated near-field pattern for the test geometry shown.

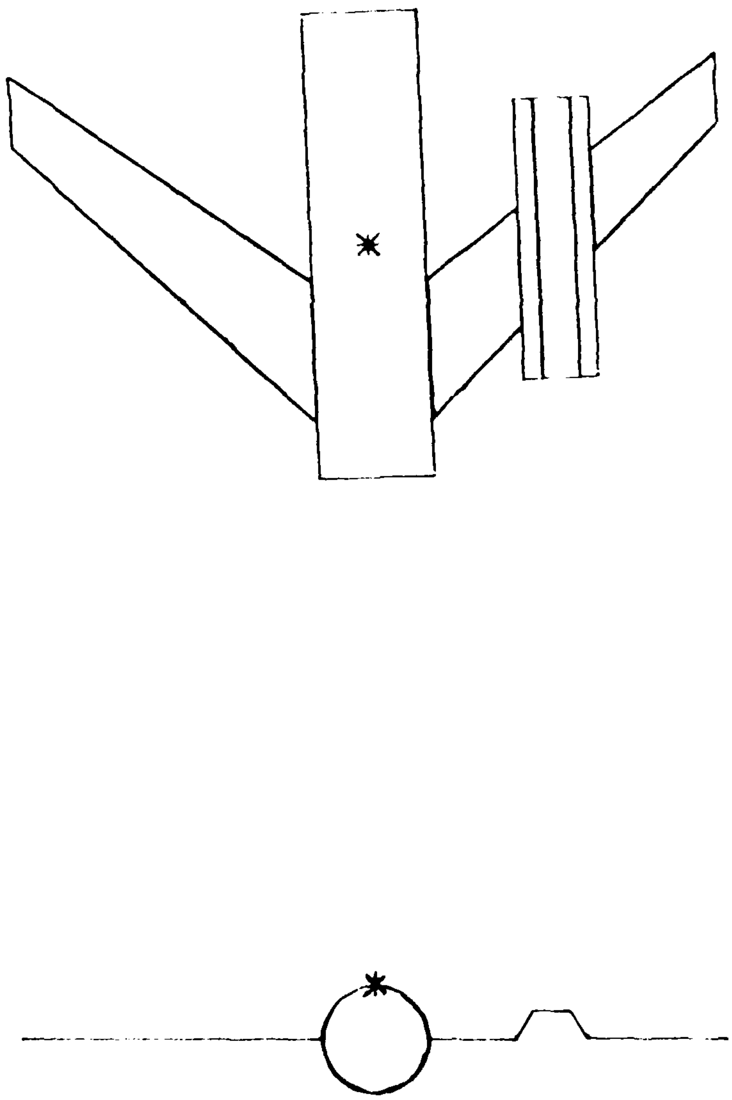

Figure 15. Test geometry with flat-plate engine model.

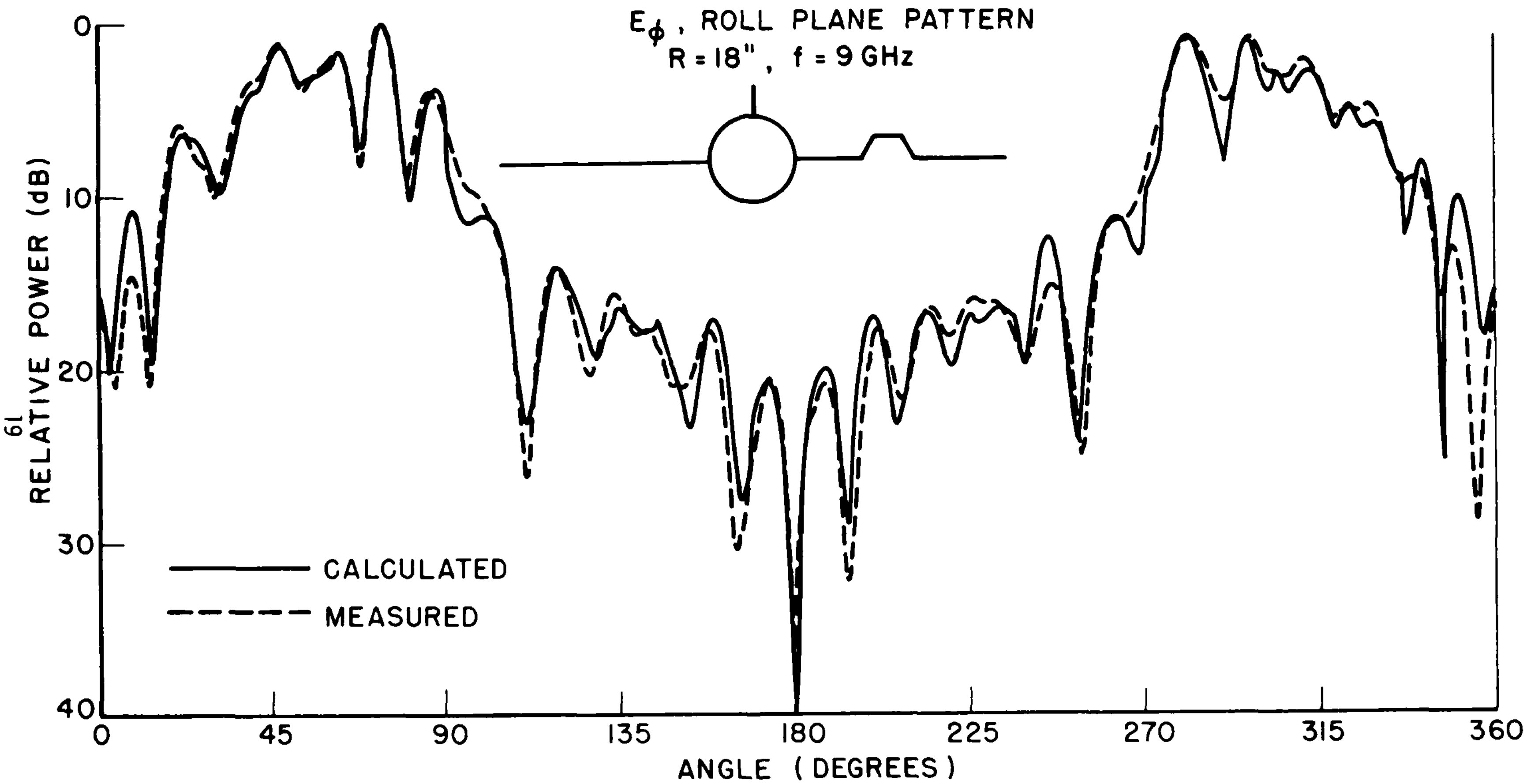

Figure 16. Comparison of measured and calculated near-field pattern for the test geometry shown.

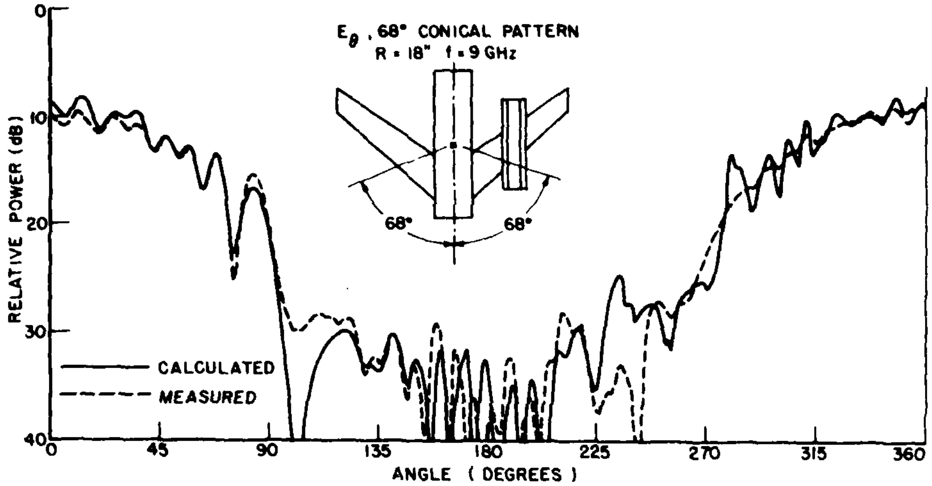

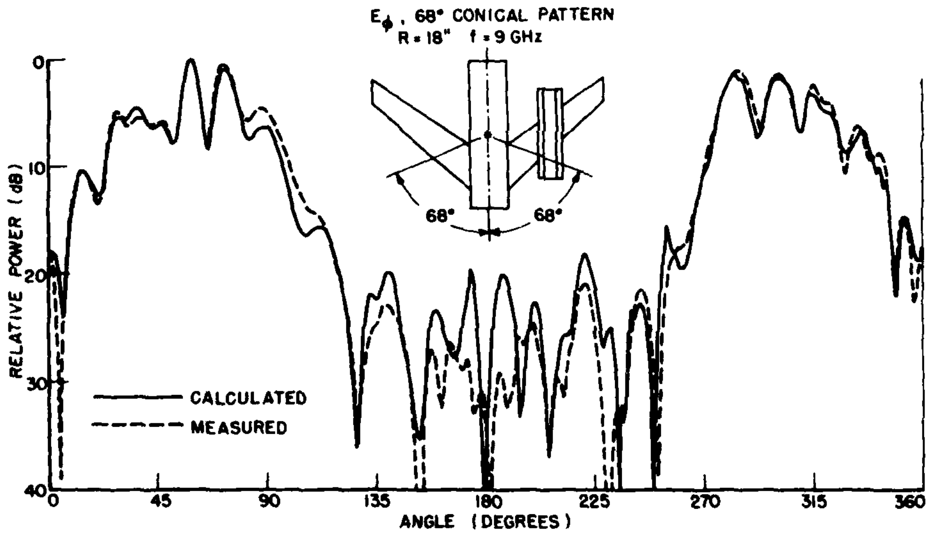

Figure 17. Comparison of measured and calculated near-field patterns for the test geometry. Note that the engine is simulated by flat plates.

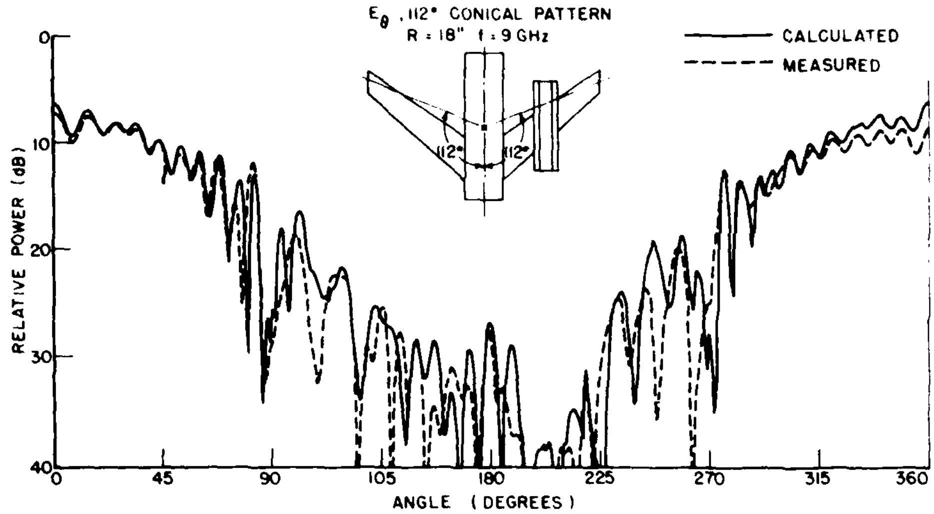

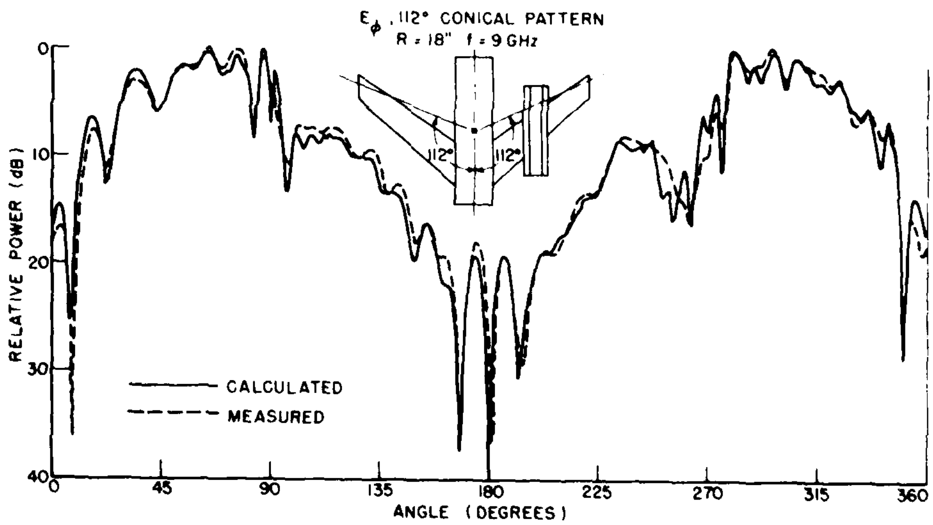

Figure 18. Comparison of measured and calculated near-field patterns for the test geometry. Note that the engine is simulated by flat plates.

REFERENCES

1. W.D. Burnside, N. Wang and E.L. Pelton, "Near Field Pattern Computations for Airborne Antennas," Report 784685-4, June 1978, The Ohio State University ElectroScience Laboratory, Department of Electrical Engineering; prepared under Contract N00019-77-C-0299 for Naval Air Systems Command.

2. K.W. Burgener and W.D. Burnside,"Analysis of Private Aircraft Antenna Patterns," Report 710964-2, January 1979, The Ohio State University ElectroScience Laboratory, Department of Electrical Engineering; prepared under Grant NSG-1498 for National Aeronautics and Space Administration.

APPENDIX A

1) Input data for the test geometry as shown in Figure 1.

```
F,F,F,F,1
5ØØ.,9.
2.5,2.5,2.5,2.5
Ø.,Ø.,Ø.
Ø.,Ø.
.25,.5,Ø.,.25,3
9Ø.,Ø.,3ØØ,1
Ø.,Ø.
1
PLATE NO. 1;RECTANGULAR PLATE ATTACHED TO CYLINDER
4,1,Ø.,Ø.,Ø.
1.7678,1.7678,-8Ø.
1.7678,4.2678,-8Ø.
1.7678,4.2678,8Ø.
1.7678,1.7678,8Ø.
1
1,4,1,2
```

2) Input data for the test geometry as shown in Figure 4.

```
F,F,F,F,1
5ØØ.,9.
2.5,2.5,2.5,2.5
Ø.,Ø.,Ø.
Ø.,Ø.
.25,.5,Ø.,.25,3
9Ø.,Ø,3ØØ,1
Ø.,Ø.
2
PLATE NO. 1;RECTANGULAR PLATE ATTACHED TO CYLINDER
4,1,Ø.,Ø.,Ø.
1.7678,1.7678,-8Ø.
1.7678,4.2678,-8Ø.
1.7678,4.2678,8Ø.
1.7678,1.7678,8Ø.
PLATE #2; RECTANGULAR PLATE ATTACHED TO PLATE #1
4,F,Ø.,Ø.,Ø.
1.7678,4.2678,-8Ø.
5.,7.5,-8Ø.
5.,7.5,8Ø.
1.7678,4.2678,8Ø.
2
1,4,1,2
1,4,2,2
```

3) Input data for the test geometry as shown in Figure 9.

```
F,F,F,T
24.,9.
2.5,2.5,2.5,2.5
0.,0.,0.
3.825,0.
.25,.5,0.,.25,3
90,90,1,0,500,1
0.,0.

5
PLATE NO. 1;RIGHT WING BETWEEN CYLINDER AND ENGINE
4,T,0.,0.,0.
0.,2.5,-4.
0.,7.5,-4.
0.,7.5,4.
0.,2.5,4.
PLATE NO. 2;ENGINE PLATE FACING CYLINDER
4,F,0.,0.,0.
0.,7.5,-4.
1.353,8.281,-4.
1.353,8.281,4.
0.,7.5,4.
PLATE NO. 3;ENGINE PLATE PARALLEL TO WING
4,F,0.,0.,0.
1.353,8.281,-4.
1.353,9.906,-4.
1.353,9.906,4.
1.353,8.281,4.
PLATE NO. 4;ENGINE PLATE FACING AWAY FROM CYLINDER
4,F,0.,0.,0.
1.353,9.906,-4.
0.,10.0875,-4.
0.,10.0875,4.
1.353,9.906,4.
PLATE NO. 5;RIGHT WING TIP
4,F,0.,0.,0.
0.,10.0875,-4.
0.,17.5,-4.
0.,17.5,4.
0.,10.0875,4.
4
3,4,2
3,2,4
4,4,2
5,4,2
```

4) Input data for the test geometry as shown in Figure 15.

```
F,F,F,1
18.,9.
2.5,2.5,2.5,2.5
Ø.,Ø.,Ø.
Ø.,Ø.
.25,.5,Ø.,.25,3
112,112,34,Ø,300,1
Ø.,Ø.
6
PLATE NO. 1;LEFT WING SECTION BETWEEN CYLINDER AND ENGINE
4,T,Ø.,Ø.,Ø.
Ø.,-2.5,7.55
Ø.,-6.5,3.7
Ø.,-6.5,-1.33
Ø.,-2.5,1.58
PLATE NO. 2;WING ENGINE PLATE NEAREST CYLINDER
6,F,Ø.,Ø.,Ø.
Ø.,-6.5,6.
1.375,-7.3,6.
1.375,-7.3,-6.
Ø.,-6.5,-6.
Ø.,-6.5,-1.33
Ø.,-6.5,3.7
PLATE NO. 3;WING ENGINE PLATE PARALLEL TO WING
4,F,Ø.,Ø.,Ø.
1.375,-7.3,6.
1.375,-8.9,6.
1.375,-8.9,-6.
1.375,-7.3,-6.
PLATE NO. 4;WING ENGINE PLATE AWAY FROM CYLINDER
6,F,Ø.,Ø.,Ø.
1.375,-8.9,6.
Ø.,-9.7,6.
Ø.,-9.7,.55
Ø.,-9.7,-3.72
Ø.,-9.7,-6.
1.375,-8.9,-6.
PLATE NO. 5;LEFT WING TIP
4,F,Ø.,Ø.,Ø.
Ø.,-9.7,.55
Ø.,-15.125,-4.68
Ø.,-15.15,-7.7
Ø.,-9.7,-3.72
PLATE NO. 6;RIGHT WING
4,T,Ø.,Ø.,Ø.
Ø.,2.5,1.58
Ø.,15.15,-7.7
Ø.,15.125,-4.68
Ø.,2.5,7.55
```

04

D